

# Imaging, Understanding, and Controlling of Nanoscale Materials Transformations

Haimei Zheng

Materials Sciences Division, Lawrence Berkeley National Laboratory, and Department of Materials Science and Engineering, University of California, Berkeley, California 94720, United States

The development of liquid cells for transmission electron microscopy (TEM) enabled breakthroughs in our ability to follow nanoscale structural, morphological, or chemical changes during materials growth and applications. Time-resolved high-resolution imaging and chemical analysis through liquids opened the opportunity to capture nanoscale dynamic processes of materials, including reaction intermediates and the transformation pathways. In this article, a series of work is highlighted with topics ranging from liquid cell developments to in situ studies of nanocrystal growth and transformations, dendrite formation and suppression of lithium dendrites through in situ characterization of the solid electrolyte interphases (SEI) chemistry. The understanding garnered is expected to accelerate the discovery of novel materials for applications in energy storage, catalysis, sensors and other functional devices.

Keywords: Nucleation and growth, self-assembly, electrode-electrolyte interfaces, Liquid cells, liquid phase TEM

A fundamental understanding of materials transformations is critical to designing novel materials and the applications of materials in functional devices. Materials often experience structural, morphological, or chemical transformations in response to an external stimulus. Presently, it remains challenging to make useful predictions on the transformation pathways of nanomaterials using statistical theories. Nanoscale systems and their transformations can be dominated by inhomogeneity and fluctuations. Direct measurement of individual events using in situ high-resolution imaging often becomes necessary for achieving a basic understanding of the underlying processes and governing factors. While challenges remain in reliable, real-time imaging of materials transformations in liquids at small length and time scales, progresses have been made, as highlighted in the current paper.

Liquid cell TEM (also called liquid phase TEM) has attracted broad interests in recent years.<sup>1</sup> Recent developments have extended earlier liquid cell techniques to incorporate a wide range of capabilities, including high spatial resolution, real-time chemical analysis using energy dispersive x-ray spectroscopy (EDS) and electron energy loss spectroscopy (EELS). These advances enabled us to resolve some of the issues critical to an understanding of nanoscale transformation mechanisms. Examples include the studies of defect evolution in nanometer-sized crystals and of multicomponent material systems<sup>2,3,4,5</sup> where chemical analysis is essential. Recent liquid cell development<sup>6,7</sup> enabled unprecedented spatial resolution ( $\sim 2$  Å) in comparison to earlier techniques (1 to 5 nm).<sup>8,9</sup> Additionally, direct EDS through liquid cell samples opened a range of opportunities. Central to this development is the use of thin membranes. The subsequent work on liquid cells with thin membranes enabled spatial resolutions down to the atomic scale<sup>10-14</sup> and high resolution imaging of biological samples.<sup>15</sup> The new design also allows the study of electrochemistry in liquid cells with various electrode configurations.<sup>4,16,17</sup> Today, the high-resolution liquid cells are compatible with EELS, EDS, and atomic resolution scanning TEM

(STEM) analysis. In addition, thermal heating of a liquid cell for in situ TEM was accomplished, which is important for studying thermally induced nucleation and growth of nanoparticles (rather than electron beam induced processes).<sup>18</sup> The improved capability for liquid-cell studies also took advantage of recent advances in TEM, including aberration-corrected electron optics, fast electron detectors, and advanced image analysis. It is important to note that collaboration with industrial partners has greatly promoted the development of liquid cell technique along with electron microscopy instrumentation.<sup>13,19,20</sup>

The liquid cell TEM is a powerful platform to tackle many challenging problems. It facilitated a series of discoveries through detailed studies of nucleation, growth, and self-assembly of nanoparticles, electrode-electrolyte interfaces, catalysis, and beyond. Other areas of study include nanoscale chemical reactions, solid-liquid-gas interfaces, catalysis, and biological samples.

In this paper, I highlight the liquid cell development and its associated work with a focus on non-spherical nanoscale materials, including the growth and transformations of Pt-Fe nanowires,<sup>2</sup> facet development of Pt nanocubes,<sup>13,21</sup> 2-dimensional (2D) nanosheet formation with 3-dimensional (3D) nanoparticles as the intermediates,<sup>14</sup> reversible giant deformation of PbSe nanocrystals during superlattice transformations,<sup>11</sup> and Li dendrites formation.<sup>4,22</sup> Not only do these material systems have unique anisotropic properties,<sup>23,24</sup> they are also ideal systems for exploring non-equilibrium behaviors at the nanoscale, in which a small perturbation can drive them out of equilibrium. To this end, direct observations with high spatial and temporal resolution are necessary for yielding critical insights to a range of related questions. These include how a system responds to perturbations, and what are the governing rules for a system to evolve away from its initial thermodynamic equilibrium. Coupled with theoretical calculations, these fundamental studies foster the discovery of novel materials and promote their real-world applications in functional devices.

This paper is adapted and extended from the presentation I gave at the MRS Medal Award session of the 2019 MRS Fall Meeting. It is my hope that researchers from materials science to physics, chemistry, and engineering, find the materials presented informative and useful.

### **Development of liquid cells allowing high-resolution imaging and chemical analysis**

The challenges of liquid phase TEM imaging arise largely from the liquid cell being too thick to achieve high resolution. Previously, nitrocellulose thin films,<sup>25</sup> aluminum thin films<sup>26</sup> and thick SiN<sub>x</sub> membrane over 50 nm in thickness were typically used; and liquid cell fabrication features the stacking or gluing two chips together. Making ultra-thin freestanding membranes and controlling the liquid thickness are some of the key attributes to recent developments. These were achieved by using low-stress silicon nitride, SiN<sub>x</sub> ( $x < 4/3$ ), 25 nm in thickness on a thinner silicon wafer (100 μm thick as compared to the standard 500 μm thick standard wafer). Even thinner SiN<sub>x</sub> membranes have been developed and used more recently. A unique problem associated with the use of thin wafers is that they are too fragile to be processed using standard nanofabrication processes. To overcome this problem, one solution is to bond a thin wafer first to a standard 500 μm wafer with photoresist, thus batch fabrication of liquid cells with automated lithography patterning can be accomplished (**Figure 1a**). To control the liquid thickness inside the cell, a thin Sn spacer (70-100 nm) may be deposited by thermal evaporation on the bottom chip of the cell and bottom chip can be bonded with the top chip. The thin wafer design minimizes the attenuation of x-ray signals in EDS (**Figure 2**). The self-contained liquid cells (**Figure 1c**) with dimensions typically of 2.6 mm × 2.6 mm and 200 μm in thickness fit well into a standard TEM holder.<sup>6,7</sup>

Electrochemical liquid cells may be fabricated by incorporating patterned electrodes (**Figure 1e-f**). Various of metals (e.g., Au, Ti, and Pt) may be used as the electrode materials.<sup>16, 3, 22, 27</sup>, and they may be electrically connected to the electric pads on the TEM holder with Au or Al wires. Here, the TEM holder must be specially designed to enable electrochemical biasing. EDS chemical analysis is also possible with these thin electrochemical liquid cells. For most of the studies on deposition of alkali metals on the electrode, high resolution imaging is possible but low dose imaging is often necessary to avoid electron beam damage, as will be elaborated later.

Superior high-resolution imaging has been accomplished with a range of newer membranes and 2D materials ranging from carbon films<sup>10, 11</sup> to MoS<sub>2</sub> combined with graphene<sup>12</sup> (**Figure 1g-i**); lipid nanoreactors<sup>28</sup> (**Figure 1g**), on the other hand, offer unique opportunities for study of controlled nanochemistry and nanoscale chemical reactions.

### **In situ high resolution tracking of colloidal nanoparticle growth and transformations**

The ability to directly monitor colloidal nanoparticle transformations with high resolution opens the opportunities to uncover their growth and transformation mechanisms. Many nanoparticles show no distinct facets (**Figure 2a-c**). A group of nanoparticles with certain shape and facets, such as nanowires, nanosheets, and nanocubes, has attracted significant interests due to their shape-dependent properties. Synthesis of nanoparticles with controlled shapes has been achieved recently.<sup>29</sup> However, our understanding of the shape control mechanisms remains limited in many nanoparticle systems.

The conventional way of investigating nanocrystal growth is by ex situ measurements, e.g., by periodically taking out nanoparticles from the solution during synthesis, drying them and examining them under TEM. The drawbacks of ex situ measurements are the possible structural changes during sample preparation and the need to infer crystal growth between the examining points. Direct imaging during synthesis resolves this problem, as we can track the trajectories of individual nanoparticle growth and capture the intermediate states on the fly.

Liquid cell imaging can provide valuable insights into the growth mechanisms of 1D nanowires from quantum-dots as the building blocks. **Figure 3a** shows the sequential images of the growth of a single Pt-Fe nanorod from a molecular precursor solution. Nanoparticles were formed initially. They subsequently attached together to form a nanowire, followed by atomic-level structural rearrangement between the nanoparticles eventually leading to the formation of a single crystal Pt<sub>3</sub>Fe nanowire.<sup>2</sup> The role of ligands in the nanoparticle shape evolution is revealed through theoretical simulation coupled with a series of control experiments.<sup>2, 30, 21</sup> With advanced image analysis, it is possible to capture the interaction energetics during nanoparticle self-assembly.<sup>30</sup>

Pt nanocube formation has been studied using liquid cell TEM (**Figure 3d-f**).<sup>13</sup> For the shape evolution of nanocrystals, Wulff construction<sup>31, 32</sup> is often used to explain their growth. For instance, the high-energy facet grows faster than the low-energy facets. In other words, the fast growing facets are eventually replaced by low energy facets.<sup>29, 33</sup> Surfactant ligands however modify the facet energy, thus influencing the relative growth rate of different facets and altering the final shape of a nanocrystal.<sup>34, 35</sup> An in situ study of Pt nanocube growth demonstrated that the facet development can deviate from the Wulff construction. As shown in **Figure 3e**, the growth rates of all low energy index facets, {100}, {110} and {111}, are similar until the {100} facets stop growing at about 2.5 nm ( $d_c$ ). The {110} facets continue to grow until an edge is formed, whereas the growth of {111} facets fill the corners of the nanocube. Density functional theory (DFT) calculation revealed that the different mobilities of the ligands on the different facets play

an important role here. Specifically, the mobility of ligands is several orders of magnitude lower on the {100} than the {111} facets, thus retarding the growth of the {100} facets. A selective facet arrested shape control mechanism, mediated by the ligand mobility on different facets, is thus proposed from the complementary theoretical calculations and experiments. Interestingly, the growth of nanocrystals was found to be largely stochastic when they are smaller than a critical size ( $d_c = 2.5$  nm), below which no obvious differences in the growth rate could be observed.

Drastic shape evolution was also observed in the growth of cobalt oxide or cobalt nickel oxide nanoparticles (**Figure 3g-i**). Nanoparticles are formed first from a precursor solution. And, rather unexpectedly, they transform into nanosheets after they reach a critical size (**Figure 3g**). The phenomenon differs from the previously reported 2D nanosheet formation through oriented attachment of primary 3D nanocrystals<sup>36, 37</sup> or the “soft template”-assisted growth of 2D nanostructure.<sup>38-40</sup> As illustrated in **Figure 3g**, the 3D-to-2D transformation involves thinning down at the edges of the nanoparticles first followed by the formation of a uniform single crystal nanosheet. Clearly, such a growth behavior cannot be satisfactorily explained by the conventional growth theory based on the competing surface energy and volume energy. Rather, the observed phenomenon must be explained by considering a shape factor and introducing an edge energy.<sup>14</sup> For the cobalt oxide, the critical size was found to be about 3.8 nm, above which the 3D-to-2D transition is accompanied by a decrease in the total system energy. For the nickel oxide, however, the critical size was found to be substantially larger,  $> 10$  nm. For this reason, it maintains 3D growth without the 3D-to-2D transition as observed in the in situ experiments.

Individual PbSe nanocrystals were observed to experience shape changes during superlattice transformations. These “hidden” shape changes introduce defects, which is an issue since they can impact the properties of the solar cell devices.<sup>11</sup> The study used a unique carbon film liquid cell (**Figure 1g**) in which the as-synthesized PbSe nanocrystals capped with oleate ligands in a toluene solution was drop casted on one carbon film. To complete the liquid cell, a droplet of ligand exchange solution (ethylene glycol (EG) or EG with ethylenediamine (EDA)) was loaded on the other carbon film. Small pockets of liquids formed in the liquid cell, enabling in situ observation of the PbSe nanocrystal superlattice transformations. Observation revealed that PbSe nanocrystals change shape when interacting with neighboring particles and the deformation was dependent on the chemistry during ligands exchange (**Figure 4a**). When oleate ligands were removed from the nanoparticle surface by EG, negligible changes of individual nanocrystals were observed. In contrast, a small amount of EDA (EDA:EG=1:1000) in the ligand exchange solution was found to produce large shape changes (up to 40%). In situ movies show much faster superlattice transformations (by an order of magnitude) when EDA was applied. Molecular dynamics simulation suggests that the electrostatic dipolar interactions between nanocrystals, arising from the fast ligand removal, played a major role in the observed reversible shape changes. The deformation of individual PbSe nanocrystals introduces defects in the final superlattice. More defects, such as lower degree of connectivity and higher degree of misorientation, were seen in the superlattice formed by ligand exchange with EDA than that formed with pure EG (**Figure 4c-d**). Further in situ study resolved the necking formation mechanism at the atomic level and revealed the origin of defects in PbSe superlattice transformations.<sup>41</sup>

## **In situ study of dendrite formation at the nanoscale**

### *Understanding nanodendrite pattern formation*

Dendritic materials are widely found both in nature and through laboratory synthesis.<sup>42</sup> Their formation mechanisms have been explored theoretically.<sup>43-49</sup> Using liquid cell TEM with

fine control of the growth conditions and advanced data collection and image analysis, the growth mechanism of iron oxide nanodendrites has been studied with a focus on validating the applicability of available theories for nanoscale systems. Iron oxide nanodendrites grew predominantly in two dimensions on the membrane of a liquid cell (**Figure 5a**). Tracking the trajectories of their morphology development reveals the relationship between the tip curvature and growth rate, tip splitting relative to instabilities, and the effects of precursor diffusion and depletion on the morphology evolution. Interestingly, the dendritic morphology evolution observed during the growth of iron oxide nanodendrites was remarkably consistent with existing theoretical predictions, despite occurring at the nanoscale.<sup>50, 51</sup>

Interests in metal dendrites stems from the fact that their growth is a primary cause for short-circuit failures in rechargeable batteries and other electronic devices. In a study of the crystallization and morphology evolution of lead dendrites,<sup>16</sup> we observed dendrite growth through tip-splitting and dissolution of dendrites with mass loss when electric biasing was reversed (**Figure 5c**). Through detailed control experiments, a growth model may be deduced. The electrochemically reduced lead atoms form nanograins on the electrode. They subsequently aggregate into clusters and eventually form dendritic structure. In situ study of Li dendritic growth with liquid phase TEM was challenging because of the use of air/moisture sensitive electrolyte, and alkali metals being electron beam sensitive.<sup>22</sup> Nevertheless, the deposition and dissolution of Li dendrites were observed in situ for the first time using a commercial electrolyte for Li-ion batteries (**Figure 5d, 5f**). More discussion is provided in what follows.

#### *Understanding and controlling of Li dendrite growth through in situ chemical analysis*

Alkali metal (e.g., Li and Na) plating and stripping have been studied using liquid cell TEM<sup>3, 17, 22</sup> with an emphasis on analysis of the role of solid–electrolyte interphase (SEI)<sup>3, 4</sup>. As a passivation interfacial film formed from the reduction of the electrolyte, SEI plays an important role in the cycle stability of Li-ion batteries. Previously, efforts have been devoted to an understanding of the nature of SEI, primarily through ex situ spectroscopy or microscopy, such as, FTIR, Raman Spectroscopy, atomic force microscopy, x-ray photoelectron spectroscopy, and scanning tunneling microscopy.<sup>52, 53</sup> In situ observations are beneficial as it avoids complications due to sample exposure to air and moisture. In-situ characterization has been attempted using x-ray scattering,<sup>54</sup> and neutron reflectometry.<sup>55</sup> In situ electron microscopy imaging with nanoscale chemical analysis complements these studies.<sup>56</sup> Liquid phase TEM observations and nanobeam diffraction of SEI on the electrode revealed that the SEI layer contained LiF nanocrystals distributed in an amorphous matrix,<sup>3, 4</sup> in contrast to the previous understanding of a denser layer of inorganic components adhering to the electrode with a porous organic outer layer exposing to electrolyte.<sup>57-59</sup> Since the Ti electrode is not reactive with the LiPF<sub>6</sub>/EC/DEC electrolyte, the formation of SEI should be stepwise from preferential reduction of certain electrolyte components.<sup>3</sup> In the contrary, the Li metal electrode reacts with the electrolyte directly, leading to instantaneous SEI formation. For this reason, the reduction of electrolyte components should be indiscriminate to all species.<sup>3</sup>

Further advances of in situ study of electrochemical liquid cells allowed the mapping of spatially resolved SEI chemistry on individual lithium nanograins.<sup>4</sup> The observation revealed that Li dendrites can be suppressed by a cationic polymer coating on the electrode (**Figure 5 e-h**), thus uncovering a potential path to Li dendrite suppression.

#### **Electron beam effects**

The high energy electron beam is known to interact with liquids, causing molecular dissociation, ionization, and other chemical reactions. Concerns about sample damage due to electron beam exposure have been discussed throughout the history of electron microscopy development.<sup>60</sup> Recently, there have been an increased number of studies on this problem especially for beam sensitive materials in liquids.<sup>61</sup> There have also been reports about simulation of radiolysis induced damages of water<sup>62</sup> and organic molecules.<sup>63</sup> Real-time time-dependent density functional theory (rt-TDDFT) calculations revealed the strong competition among different dissociation paths in C<sub>2</sub>H<sub>6</sub>O<sub>2</sub> radiolysis.<sup>63</sup> Obviously, blocking the dissociation paths during electron microscopy imaging may reduce the electron beam damage, even though radiolysis damage to a liquid solution can be rather complex. Many factors must be considered, including the electron beam energy, molecules being studied and their competing chemical reactions. While no universal solution exists, lowering the electron beam current density reduces the electron beam effects. For example, low dose imaging has been applied to electrochemical studies<sup>3, 4, 16, 17, 22</sup> and no discernible reactions should be observed before applying an electric bias. In the study of nanocrystal growth and transformations, strong electron beam intensity was often needed, in which case, control experiments would become critical to observing and isolating the beam damage effects.

For example, in situ imaging of PbSe nanocrystals in a commercial flow cell showed fast deterioration of the nanocrystals to form liquid-like domains.<sup>64</sup> A series of control experiments, including liquid cell TEM imaging of PbSe nanocrystals in water and in situ environmental TEM imaging of PbSe nanocrystals in 1 bar oxygen, suggest that electron beam damage of PbSe nanocrystals is coupled with their exposure to oxygen and moisture. Indeed, using the self-contained carbon-film liquid cell, PbSe nanocrystals were found to be stable under extended strong electron beam illumination. By eliminating the exposure of PbSe to oxygen and moisture, ligand exchange reactions with different solution chemistry were achieved with high resolution and in real time.<sup>11</sup>

### **Understanding of materials transformations accelerates materials discovery**

With the fundamental understanding of nanoscale materials growth and transformations garnered from in situ studies, materials may be designed for achieving special functions. For example, a series of functional materials was prepared through laser synthesis involving non-equilibrium phonon induced reactions.<sup>65-67</sup> Nanoporous metal-organic composites were designed and prepared recently, showing nearly 100% selectivity of CO production over H<sub>2</sub> generation from CO<sub>2</sub> reduction reaction. Tandem catalysts prepared by incorporating Rh or Ag nanoparticles into the metal-organic composites, on the other hand, produced formic and acetic acids. Remarkably, laser synthesis significantly shortens the growth processes, from 24+ hours with the conventional solvothermal method to 30min-2 hours.

### **Conclusions**

With the development of in situ liquid cell TEM, unprecedented advances in high-resolution imaging and chemical analysis have been made for a wide range of problems involving nanoscale materials growth and transformations. These advances opened many opportunities to resolve dynamic processes of nanoscale materials that were unreachable previously. This paper highlights some examples of liquid phase TEM studies of nanoscale materials, from one-dimensional nanocrystals to faceted nanocrystals, 2D nanosheets and superlattice transformations. Other applications discussed include nanodendrite formation and Li dendrite suppression by

resolving nanoscale structure and chemistry of SEI. Clearly, the advances can accelerate materials discovery and extend materials research to other fields of research from chemistry to physics and biology.

### **Conflicts of Interest**

The author declares no competing financial interests.

### **Data availability**

Data are available in the online version of this paper. Data that support the findings of this study are available from the author upon reasonable request.

### **Acknowledgments**

I would like to thank the current and previous members of my research group for their dedication and effort in research. I would especially like to thank my graduate students, Junyi Shangguan and Daewon Lee, for their assistance in preparing references and figures and Dr. Yu Wang for proof reading of this article. The work was supported by the U.S. Department of Energy (DOE), Office of Science, Office of Basic Energy Sciences (BES), Materials Sciences and Engineering Division under Contract No. DE-AC02-05-CH11231 within the KC22ZH program. Work at the Molecular Foundry of Lawrence Berkeley National Laboratory (LBNL) was supported by the Office of Science, Office of Basic Energy Sciences, of the U.S. Department of Energy under Contract No. DE-AC02-05CH11231.

## Figure Captions

Figure 1. The development of self-contained liquid cells allowing high resolution and chemical analysis capabilities. (a) A thin Si wafer with the thickness of 100  $\mu\text{m}$  was used. It was bonded to a standard wafer with the thickness of 500  $\mu\text{m}$ , thus programmed lithographical patterning for batch fabrication can be achieved. (b) A photolithography mask for batch fabrication of the liquid cells. (c) A photograph of regular liquid cells. (d) A photograph of electrochemical liquid cells. (e) A schematic illustration showing that electrodes were made on the bottom chip, liquid reservoirs and Sn spacer (blue) were made on the top chip of a liquid cell. (Adapted with permission from Ref.3. Copyright 2015 American Chemical Society.) (f) We developed a TEM holder with electrical biasing capability for the electrochemical cells in (d). (g) A thin carbon film liquid cells enabling controlled reactions in PbSe superlattice transformations. (Adapted from Ref.11.) (h) In a  $\text{MoS}_2$  liquid cell,  $\text{MoS}_2$  2D film serves as a functional substrate as well the supporting membrane. (Adapted with permission from Ref.12. Copyright 2019 American Chemical Society.) (i) Lipid nanoreactors were developed. (Adapted from Ref. 28 with permission from the Royal Society of Chemistry.)

Figure 2. The initial work on high resolution imaging and chemical analysis of liquid cell samples. (a) High resolution images of Au nanoparticles in a liquid cell. (Adapted with permission from Ref.6. Copyright 2009 American Chemical Society.) (b) Pt nanocrystals with homogeneous particles size distributions were synthesized in a liquid cell. (c) High resolution image of a Pt nanocrystal from (b). (d) EDS spectra of a liquid cell sample corresponding to (b). ((b-d) Adapted from Ref.7 with permission from the American Association for the Advancement of Science.) (e) EELS spectra showing the liquid thickness in a liquid cell can be measured. (Reproduced from Ref.14.)

Figure 3. In situ liquid phase TEM study of non-spherical nanocrystal growth and transformations. (a) Sequential images showing the growth of a Pt nanowire by the attachment of Pt nanoparticles, which were formed from a molecular precursor solution. (b) High resolution imaging of a  $\text{Pt}_3\text{Fe}$  nanowire showing defects evolution. ((a-b) reproduced from Ref. 2.) (c) With increased concentration of surfactant ligands, Pt-Fe nanoparticles were maintained without attachment and the interaction forces and interaction energetics were calculated. (Adapted with permission from Ref.30. Copyright 2017 American Chemical Society.) (d) Sequential images showing the growth of a Pt nanocube. The simulated images (in grey) highlight the shape evolution. (e) Tracking the growth of different facets. (f) DFT calculation by considering ligand mobility and other factors. ((d-f) reproduced from Ref.13.) (g-i) The study of 2D cobalt oxide nanosheet formed with 3D nanoparticles as intermediates. (g) A schematic illustration showing the formation of 3D cobalt oxide nanoparticles and subsequent transition into 2D nanosheet. (h) High resolution images from an in situ movie showing the growth of a 2D nanosheet. (i) Theoretical calculations of the energy evolution by including a shape factor in the classical nucleation and growth theory. (Reproduced from Ref.14)

Figure 4. Liquid phase TEM study of PbSe nanocrystal deformation during superlattice transitions. (a) Reversible large deformation of PbSe nanocrystals (#11). Scale bar: 5nm. (b) Quantification of the deformation. (c) Low and high magnification TEM images showing that nearly perfect PbSe superlattice was achieved with EG as the ligand exchange solution. Scale bars: 20nm (left) and

5nm (right). (d) Comparing to (c), defects were observed with EDA in the ligand exchange solution. Scale bars: 20nm (left) and 5nm (right). (Reproduced from Ref.11.)

Figure 5. In situ study of dendrite growth allowing fundamental understanding of the dendrite formation at the nanoscale and controlling of dendrite growth in functional devices, i.e., Li ion batteries. (a) Iron oxide dendrite formed in a liquid cell overlapping with the contour map from computer tracing of the dendrite evolution. (b) Large data analysis revealed tip split arising from instabilities. (Adapted with permission from Ref.50. Copyright 2018 American Chemical Society.) (c) Electrodeposition and dissolution of Pb dendrites in an electrochemical liquid cell. (Reproduced from Ref.16) (d) Electrodeposition and dissolution of Li dendrites in an electrochemical liquid cell. (Adapted with permission from Ref.22. Copyright 2018 American Chemical Society.) (e-h) Suppressing Li dendrite formation with a cationic polymer film (PDDA) coated on the electrodes inside the liquid cell. (e) Li nanogranular growth was achieved on the electrode coated with PDDA. (f) Li dendrite growth was achieved on a bare electrode without polymer coating. (g) EDS chemical mapping of a Li nanograin with SEI on the surface. (h) EDS line scan profile showing the SEI chemistry. ((e-h) Reproduced from Ref. 4 with permission from the Royal Society of Chemistry.)

**Author biography**

Dr. Haimei Zheng

1 Cyclotron Road, 62-211

Lawrence Berkeley National Laboratory

Berkeley CA 94720

Phone: 510 486 6943

Email: [hmzheng@lbl.gov](mailto:hmzheng@lbl.gov)

Dr. Haimei Zheng is a senior scientist in Materials Sciences Division at Lawrence Berkeley National Laboratory (LBNL) and an adjunct professor in Materials Science and Engineering Department at University of California (UC), Berkeley. She earned a Ph.D. in Materials Science and Engineering from the University of Maryland, College Park. Prior to her independent research at LBNL, she was a postdoctoral fellow at UC Berkeley and LBNL.

Her research interests are centered on understanding how atomic level heterogeneity and fluctuations control physical and chemical processes of materials. By developing and applying *in situ* liquid cell electron microscopy, her group studies nucleation, growth and transformations of materials, solid-liquid (electrode-electrolyte) interfaces and catalysis. She further applies the insights garnered to novel materials engineering and device development. She received DOE Office of Science Early Career Award in 2011, LBNL Director's award for exceptional scientific achievements in 2013 and MRS Medal in 2019.

## References

1. U. Mirsaidov, J.P. Patterson and H. Zheng: Liquid phase transmission electron microscopy for imaging of nanoscale processes in solution. *MRS Bulletin* **45**, 704 (2020).
2. H.-G. Liao, L. Cui, S. Whitlam and H. Zheng: Real-time imaging of Pt<sub>3</sub>Fe nanorod growth in solution. *Science* **336**, 1011 (2012).
3. Z. Zeng, X. Zhang, K. Bustillo, K. Niu, C. Gammer, J. Xu and H. Zheng: In situ study of lithiation and delithiation of MoS<sub>2</sub> nanosheets using electrochemical liquid cell transmission electron microscopy. *Nano Letters* **15**, 5214 (2015).
4. S.-Y. Lee, J. Shangguan, J. Alvarado, S. Betzler, S.J. Harris, M.M. Doeff and H. Zheng: Unveiling the mechanisms of lithium dendrite suppression by cationic polymer film induced solid–electrolyte interphase modification. *Energy & Environmental Science* **13**, 1832 (2020).
5. K.-Y. Niu, M. Liu, K.A. Persson, Y. Han and H. Zheng: Strain-mediated interfacial dynamics during Au–PbS core–shell nanostructure formation. *ACS Nano* **10**, 6235 (2016).
6. H. Zheng, S.A. Claridge, A.M. Minor, A.P. Alivisatos and U. Dahmen: Nanocrystal diffusion in a liquid thin film observed by in situ transmission electron microscopy. *Nano Letters* **9**, 2460 (2009).
7. H. Zheng, R.K. Smith, Y.-w. Jun, C. Kisielowski, U. Dahmen and A.P. Alivisatos: Observation of single colloidal platinum nanocrystal growth trajectories. *Science* **324**, 1309 (2009).
8. M. Williamson, R. Tromp, P. Vereecken, R. Hull and F. Ross: Dynamic microscopy of nanoscale cluster growth at the solid–liquid interface. *Nature Materials* **2**, 532 (2003).
9. N. De Jonge, D.B. Peckys, G. Kremers and D. Piston: Electron microscopy of whole cells in liquid with nanometer resolution. *Proceedings of the National Academy of Sciences* **106**, 2159 (2009).
10. C. Zhu, S. Liang, E. Song, Y. Zhou, W. Wang, F. Shan, Y. Shi, C. Hao, K. Yin and T. Zhang: In-situ liquid cell transmission electron microscopy investigation on oriented attachment of gold nanoparticles. *Nature Communications* **9**, 1 (2018).
11. Y. Wang, X. Peng, A. Abelson, P. Xiao, C. Qian, L. Yu, C. Ophus, P. Ercius, L.-W. Wang and M. Law: Dynamic deformability of individual PbSe nanocrystals during superlattice phase transitions. *Science Advances* **5**, eaaw5623 (2019).
12. J. Yang, M.K. Choi, Y. Sheng, J. Jung, K. Bustillo, T. Chen, S.-W. Lee, P. Ercius, J.H. Kim and J.H. Warner: MoS<sub>2</sub> liquid cell electron microscopy through clean and fast polymer-free MoS<sub>2</sub> transfer. *Nano Letters* **19**, 1788 (2019).
13. H.-G. Liao, D. Zherebetsky, H. Xin, C. Czarnik, P. Ercius, H. Elmlund, M. Pan, L.-W. Wang and H. Zheng: Facet development during platinum nanocube growth. *Science* **345**, 916 (2014).
14. J. Yang, Z. Zeng, J. Kang, S. Betzler, C. Czarnik, X. Zhang, C. Ophus, C. Yu, K. Bustillo and M. Pan: Formation of two-dimensional transition metal oxide nanosheets with nanoparticles as intermediates. *Nature Materials* **18**, 970 (2019).
15. U.M. Mirsaidov, H. Zheng, Y. Casana and P. Matsudaira: Imaging protein structure in water at 2.7 nm resolution by transmission electron microscopy. *Biophysical Journal* **102**, L15 (2012).
16. M. Sun, H.-G. Liao, K. Niu and H. Zheng: Structural and morphological evolution of lead dendrites during electrochemical migration. *Scientific Reports* **3**, 1 (2013).

17. Z. Zeng, P. Barai, S.-Y. Lee, J. Yang, X. Zhang, W. Zheng, Y.-S. Liu, K.C. Bustillo, P. Ercius and J. Guo: Electrode roughness dependent electrodeposition of sodium at the nanoscale. *Nano Energy* **72**, 104721 (2020).
18. H.L. Xin and H. Zheng: In situ observation of oscillatory growth of bismuth nanoparticles. *Nano Letters* **12**, 1470 (2012).
19. W.-I. Liang, X. Zhang, K. Bustillo, C.-H. Chiu, W.-W. Wu, J. Xu, Y.-H. Chu and H. Zheng: In situ study of spinel ferrite nanocrystal growth using liquid cell transmission electron microscopy. *Chemistry of Materials* **27**, 8146 (2015).
20. W.-I. Liang, X. Zhang, Y. Zan, M. Pan, C. Czarnik, K. Bustillo, J. Xu, Y.-H. Chu and H. Zheng: In situ study of Fe<sub>3</sub>Pt–Fe<sub>2</sub>O<sub>3</sub> core–shell nanoparticle formation. *Journal of the American Chemical Society* **137**, 14850 (2015).
21. H.-G. Liao and H. Zheng: Liquid cell transmission electron microscopy study of platinum iron nanocrystal growth and shape evolution. *Journal of the American Chemical Society* **135**, 5038 (2013).
22. Z. Zeng, W.-I. Liang, H.-G. Liao, H.L. Xin, Y.-H. Chu and H. Zheng: Visualization of electrode–electrolyte interfaces in LiPF<sub>6</sub>/EC/DEC electrolyte for lithium ion batteries via in situ TEM. *Nano Letters* **14**, 1745 (2014).
23. A.K. Pearce, T.R. Wilks, M.C. Arno and R.K. O’Reilly: Synthesis and applications of anisotropic nanoparticles with precisely defined dimensions. *Nature Reviews Chemistry*, 1 (2020).
24. T.K. Sau, A.L. Rogach, F. Jäckel, T.A. Klar and J. Feldmann: Properties and applications of colloidal nonspherical noble metal nanoparticles. *Advanced Materials* **22**, 1805 (2010).
25. I. Abrams and J. McBain: A closed cell for electron microscopy. *Journal of Applied Physics* **15**, 607 (1944).
26. L. Marton: Electron microscopy of biological objects. *Physical Review* **46**, 527 (1934).
27. R.M. Arán-Ais, R. Rizo, P. Grosse, G. Algara-Siller, K. Dembélé, M. Plodinec, T. Lunkenbein, S.W. Chee and B.R. Cuenya: Imaging electrochemically synthesized Cu<sub>2</sub>O cubes and their morphological evolution under conditions relevant to CO<sub>2</sub> electroreduction. *Nature Communications* **11**, 3489 (2020).
28. S.B. Alam, J. Yang, K.C. Bustillo, C. Ophus, P. Ercius, H. Zheng and E.M. Chan: Hybrid nanocapsules for in situ TEM imaging of gas evolution reactions in confined liquids. *Nanoscale* **12**, 18606 (2020).
29. Y. Xia, Y. Xiong, B. Lim and S.E. Skrabalak: Shape-controlled synthesis of metal nanocrystals: simple chemistry meets complex physics? *Angewandte Chemie-International Edition* **48**, 60 (2009).
30. A.S. Powers, H.-G. Liao, S.N. Raja, N.D. Bronstein, A.P. Alivisatos and H. Zheng: Tracking nanoparticle diffusion and interaction during self-assembly in a liquid cell. *Nano Letters* **17**, 15 (2017).
31. J.W. Gibbs, H.A. Bumstead, R.G. Van Name and W.R. Longley: The collected works of J. Willard Gibbs, (Longmans, Green and Co.1902).
32. G. Wulff: On the question of speed of growth and dissolution of crystal surfaces. *Zeitschrift Fur Kristallographie Und Mineralogie* **34**, 449 (1901).
33. N. Tian, Z.-Y. Zhou, S.-G. Sun, Y. Ding and Z.L. Wang: Synthesis of tetrahedral platinum nanocrystals with high-index facets and high electro-oxidation activity. *Science* **316**, 732 (2007).

34. C.R. Bealing, W.J. Baumgardner, J.J. Choi, T. Hanrath and R.G. Hennig: Predicting nanocrystal shape through consideration of surface-ligand interactions. *ACS nano* **6**, 2118 (2012).
35. E. Ringe, R.P. Van Duyne and L.D. Marks: Wulff construction for alloy nanoparticles. *Nano letters* **11**, 3399 (2011).
36. C. Schliehe, B.H. Juarez, M. Pelletier, S. Jander, D. Greshnykh, M. Nagel, A. Meyer, S. Foerster, A. Kornowski and C. Klinke: Ultrathin PbS sheets by two-dimensional oriented attachment. *Science* **329**, 550 (2010).
37. S. Gao, Y. Sun, F. Lei, L. Liang, J. Liu, W. Bi, B. Pan and Y. Xie: Ultrahigh energy density realized by a single-layer  $\beta$ -Co(OH)<sub>2</sub> all-solid-state asymmetric supercapacitor. *Angewandte Chemie International Edition* **53**, 12789 (2014).
38. J.S. Son, X.D. Wen, J. Joo, J. Chae, S.i. Baek, K. Park, J.H. Kim, K. An, J.H. Yu and S.G. Kwon: Large-scale soft colloidal template synthesis of 1.4 nm thick CdSe nanosheets. *Angewandte Chemie* **121**, 6993 (2009).
39. S. Sun, H. Zeng, D.B. Robinson, S. Raoux, P.M. Rice, S.X. Wang and G. Li: Monodisperse MFe<sub>2</sub>O<sub>4</sub> (M= Fe, Co, Mn) nanoparticles. *Journal of the American Chemical Society* **126**, 273 (2004).
40. J.S. Son, J.H. Yu, S.G. Kwon, J. Lee, J. Joo and T. Hyeon: Colloidal synthesis of ultrathin two-dimensional semiconductor nanocrystals, (Wiley Online Library2011).
41. Y. Wang, X. Peng, A. Abelson, B.-K. Zhang, C. Qian, P. Ercius, L.-W. Wang, M. Law and H. Zheng: In situ TEM observation of neck formation during oriented attachment of PbSe nanocrystals. *Nano Research* **12**, 2549 (2019).
42. P. Meakin: *Fractals, scaling and growth far from equilibrium*. (Cambridge university press1998).
43. W.W. Mullins and R. Sekerka: Stability of a planar interface during solidification of a dilute binary alloy. *Journal of Applied Physics* **35**, 444 (1964).
44. W.W. Mullins and R.F. Sekerka: Morphological stability of a particle growing by diffusion or heat flow. *Journal of Applied Physics* **34**, 323 (1963).
45. J.S. Langer: Instabilities and pattern formation in crystal growth. *Reviews of Modern Physics* **52**, 1 (1980).
46. J. Langer: Lectures in the theory of pattern formation. *Chance and Matter*, 629 (1987).
47. D.A. Kessler, J. Koplik and H. Levine: Pattern selection in fingered growth phenomena. *Advances in Physics* **37**, 255 (1988).
48. M.B. Amar and E. Brener: Theory of pattern selection in three-dimensional nonaxisymmetric dendritic growth. *Physical Review Letters* **71**, 589 (1993).
49. A. Barbieri and J. Langer: Predictions of dendritic growth rates in the linearized solvability theory. *Physical Review A* **39**, 5314 (1989).
50. M.R. Hauwiller, X. Zhang, W.-I. Liang, C.-H. Chiu, Q. Zhang, W. Zheng, C. Ophus, E.M. Chan, C. Czarnik and M. Pan: Dynamics of nanoscale dendrite formation in solution growth revealed through in situ liquid cell electron microscopy. *Nano Letters* **18**, 6427 (2018).
51. W. Zheng, M.R. Hauwiller, W.-I. Liang, C. Ophus, P. Ercius, E.M. Chan, Y.-H. Chu, M. Asta, X. Du and A.P. Alivisatos: Real time imaging of two-dimensional iron oxide spherulite nanostructure formation. *Nano Research* **12**, 2889 (2019).
52. K. Xu: Nonaqueous liquid electrolytes for lithium-based rechargeable batteries. *Chemical Reviews* **104**, 4303 (2004).

53. P. Verma, P. Maire and P. Novák: A review of the features and analyses of the solid electrolyte interphase in Li-ion batteries. *Electrochimica Acta* **55**, 6332 (2010).
54. D. Stevens and J. Dahn: The mechanisms of lithium and sodium insertion in carbon materials. *Journal of The Electrochemical Society* **148**, A803 (2001).
55. J.E. Owejan, J.P. Owejan, S.C. DeCaluwe and J.A. Dura: Solid electrolyte interphase in Li-ion batteries: evolving structures measured in situ by neutron reflectometry. *Chemistry of Materials* **24**, 2133 (2012).
56. Y.A. Wu, Z. Yin, M. Farmand, Y.-S. Yu, D.A. Shapiro, H.-G. Liao, W.-I. Liang, Y.-H. Chu and H. Zheng: In-situ multimodal imaging and spectroscopy of Mg electrodeposition at electrode-electrolyte interfaces. *Scientific reports* **7**, 1 (2017).
57. J. Christensen and J. Newman: A mathematical model for the lithium-ion negative electrode solid electrolyte interphase. *Journal of The Electrochemical Society* **151**, A1977 (2004).
58. D. Aurbach, Y. Ein-Ely and A. Zaban: The surface chemistry of lithium electrodes in alkyl carbonate solutions. *Journal of the Electrochemical Society* **141**, L1 (1994).
59. D. Bar-Tow, E. Peled and L. Burstein: A study of highly oriented pyrolytic graphite as a model for the graphite anode in Li-Ion batteries. *Journal of the Electrochemical Society* **146**, 824 (1999).
60. S.M. Seltzer and M.J. Berger: Evaluation of the collision stopping power of elements and compounds for electrons and positrons. *The International Journal of Applied Radiation and Isotopes* **33**, 1189 (1982).
61. P. Abellan, T. Woehl, L. Parent, N. Browning, J. Evans and I. Arslan: Factors influencing quantitative liquid (scanning) transmission electron microscopy. *Chemical Communications* **50**, 4873 (2014).
62. N.M. Schneider, M.M. Norton, B.J. Mendel, J.M. Grogan, F.M. Ross and H.H. Bau: Electron–water interactions and implications for liquid cell electron microscopy. *The Journal of Physical Chemistry C* **118**, 22373 (2014).
63. Z. Cai, S. Chen and L.-W. Wang: Dissociation path competition of radiolysis ionization-induced molecule damage under electron beam illumination. *Chemical Science* **10**, 10706 (2019).
64. X. Peng, A. Abelson, Y. Wang, C. Qian, J. Shangguan, Q. Zhang, L. Yu, Z.-W. Yin, W. Zheng and K.C. Bustillo: In situ TEM study of the degradation of PbSe nanocrystals in air. *Chemistry of Materials* **31**, 190 (2018).
65. K.-Y. Niu, F. Lin, S. Jung, L. Fang, D. Nordlund, C.C. McCrory, T.-C. Weng, P. Ercius, M.M. Doeff and H. Zheng: Tuning complex transition metal hydroxide nanostructures as active catalysts for water oxidation by a laser–chemical route. *Nano Letters* **15**, 2498 (2015).
66. K.Y. Niu, L. Fang, R. Ye, D. Nordlund, M.M. Doeff, F. Lin and H. Zheng: Tailoring Transition-Metal Hydroxides and Oxides by Photon-Induced Reactions. *Angewandte Chemie* **128**, 14484 (2016).
67. K. Niu, Y. Xu, H. Wang, R. Ye, H.L. Xin, F. Lin, C. Tian, Y. Lum, K.C. Bustillo and M.M. Doeff: A spongy nickel-organic CO<sub>2</sub> reduction photocatalyst for nearly 100% selective CO production. *Science Advances* **3**, e1700921 (2017).

Figure 1.

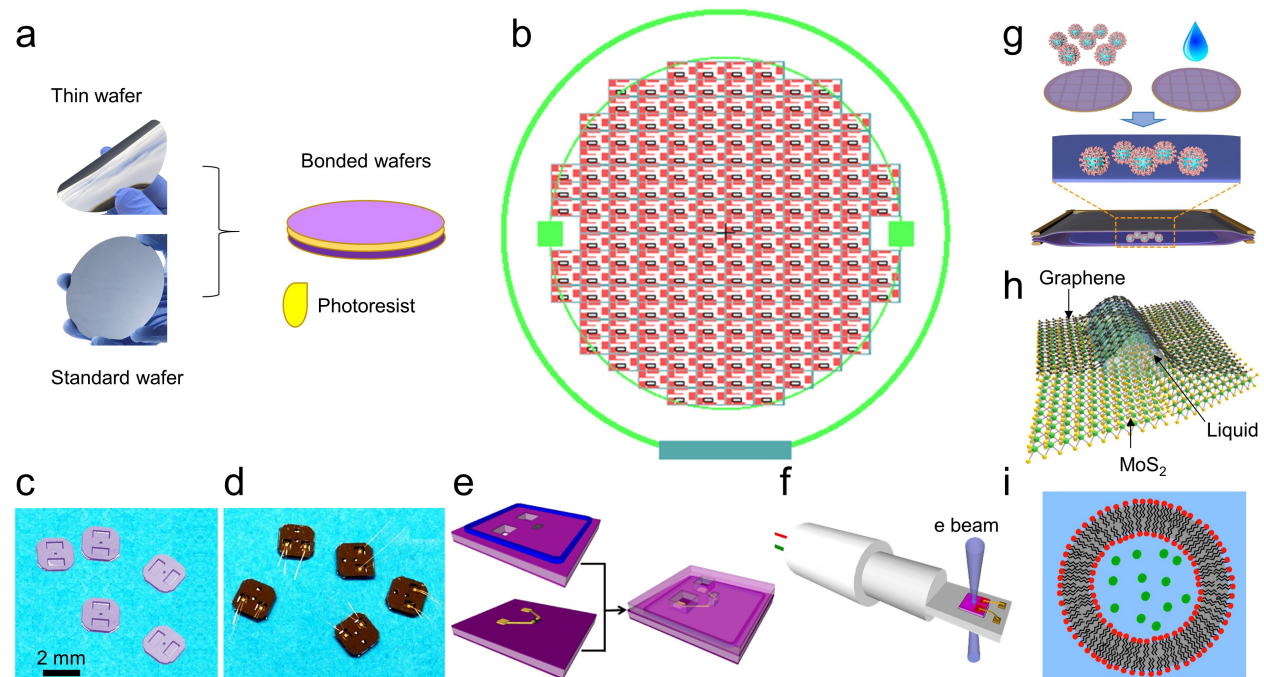


Figure 2.

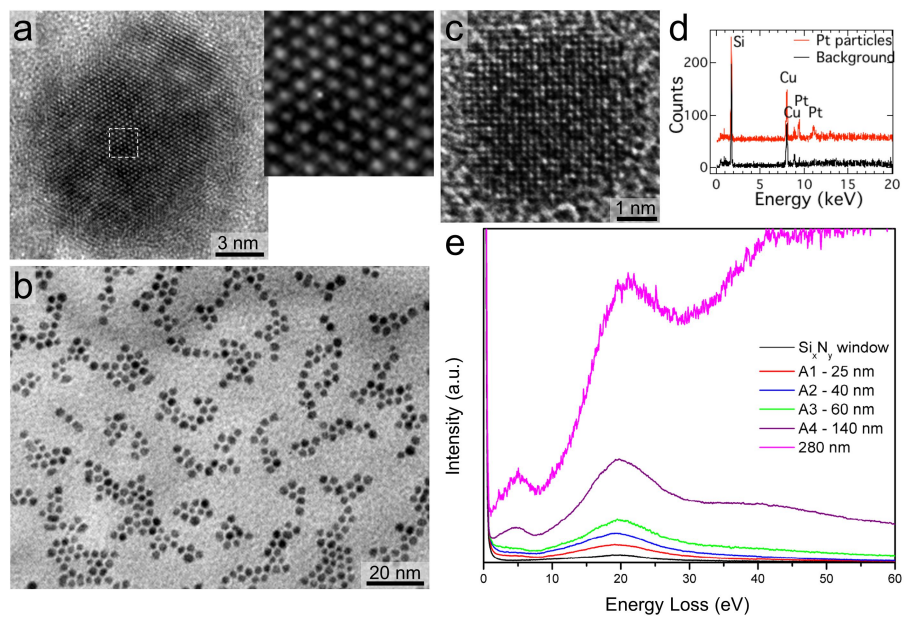


Figure 3.

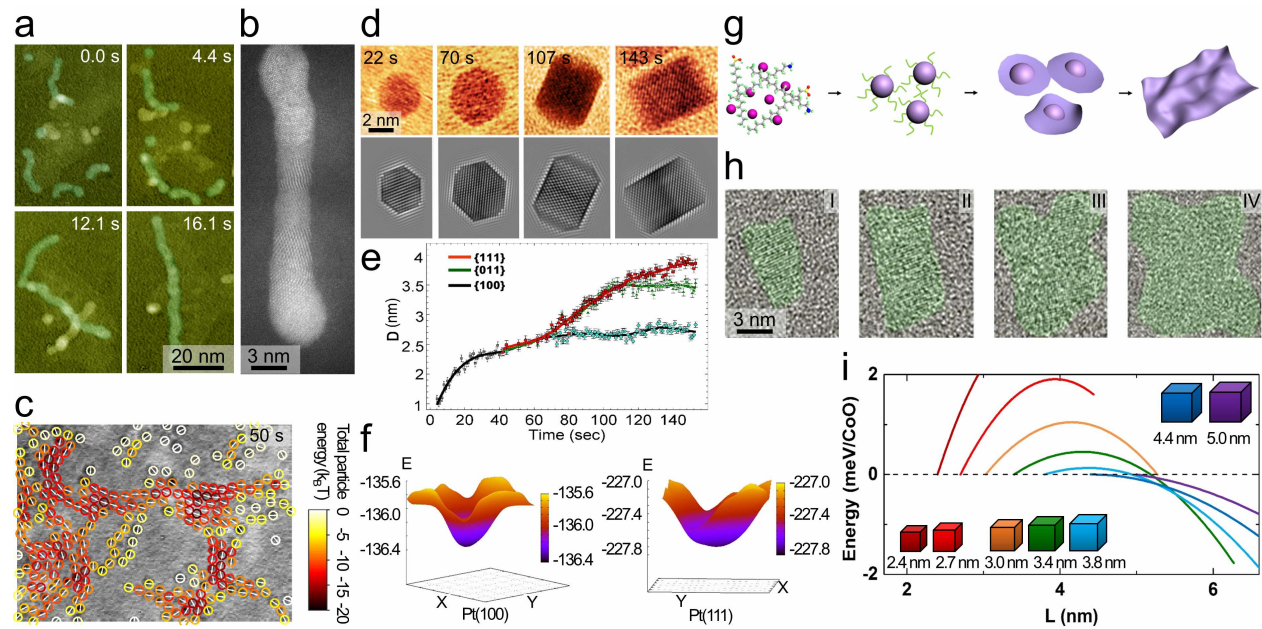


Figure 4.

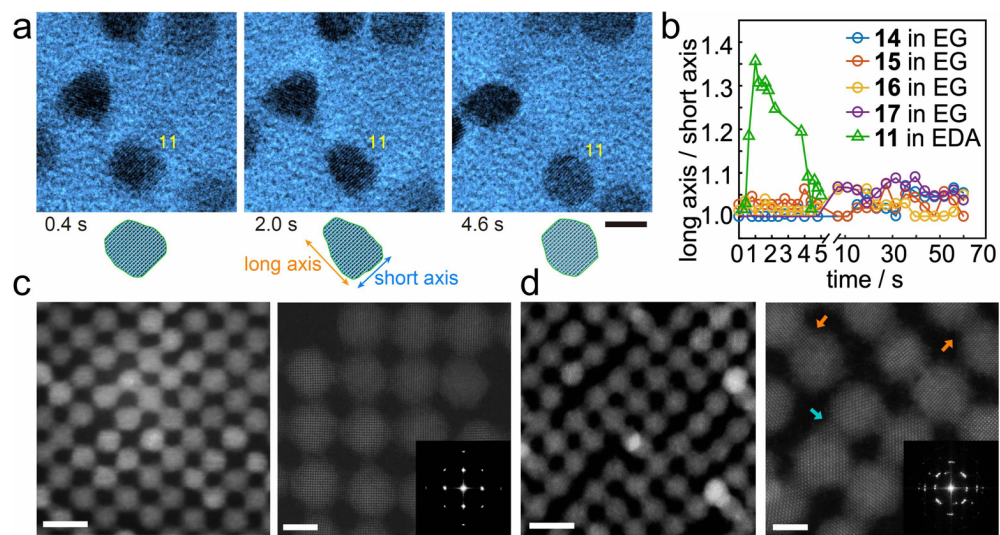


Figure 5.

